

MEHMET KALENDER
AYKUT TOPDEMİR

Department of Bioengineering,
Firat University, Elazığ, Turkey

INVESTIGATION OF THE THIN LAYER DRYING OF MICROPROPAGATED *OCIMUM BASILICUM* L.: MODELING BY DERIVED EQUATIONS, QUALITY CHARACTERISTICS, AND ENERGY EFFICIENCY

Article Highlights

- Modeling of hot air drying of micropropagated *O. basilicum* L. technique was investigated
- The derived Verma equation was the best model for drying micropropagated *O. basilicum* L. leaves
- Total phenolic, flavonoid contents and antioxidant capacity of the basil samples were typical values
- Stretch bands with alkane, aromatic, and amine/amide were observed in FT-IR spectra
- The energy efficiency analyses showed that the optimum drying temperature was 40 °C.

Abstract

This study presents the modeling of thin layer drying of micropropagated Ocimum basilicum L., some quality characteristics of the dried product, and energy consumption analysis for the dryer used. The experimental drying data obtained from a previous article were used in the statistical analyses. Modeling studies were statistically carried out using the experimental data at a 1 m/s airflow rate and a temperature of 30 °C–50 °C. The statistical analysis showed that the Verma equation was the best-fit model with the lowest chi-square (χ^2) and AIC values at all temperatures studied. From statistical analyses using derived drying models, it was found that the D9 equation having a χ^2 value of 0.0146 and an AIC value of -528.0, was the best model fitting to experimental data. The total phenolic content, flavonoid, and antioxidant capacity of dried basil samples were measured as (2.538 ± 0.029) mg GAE/g, (2.017 ± 0.088) mg quercetin/g, and (2.263 ± 0.001) mmol TEAC/100 g d.w., respectively. From FTIR spectra, dried basil samples had typical functional groups. SEM images showed that a collapse in the surface of the leaves occurred. But, this collapse is not affecting the functional groups on the surface of the leaves. From energy consumption analyses, the optimum drying temperature was found to be 40 °C. The SMER, MER, and SEC values calculated from energy consumption analysis at 40 °C were 0.0043 kg/kWh, 0.0007 kg/h, and 234.81 kWh/kg, respectively.

Keywords: micropropagation, O. basilicum L., thin-layer drying, modeling, characteristic, energy consumption.

SCIENTIFIC PAPER

UDC 66.047:635.71

Correspondence: M. Kalender, Department of Bioengineering,
Firat University, 23100, Elazığ, Turkey.
E-mail: mkalender@firat.edu.tr
Paper received: 22 July, 2022
Paper revised: 5 January, 2022
Paper accepted: 18 February, 2023

<https://doi.org/10.2298/CICEQ220722003K>

Ocimum basilicum L. (known as basil) is a multipurpose plant belonging to the Lamiaceae family. *O. basilicum* L. having aromatic and essential oil content, grows in Asia's warm, temperate, and tropical regions. It is an attractive and fragrant ornamental plant and a culinary herb [1,2]. Basil can be consumed as a fresh herb with vegetables, poultry, fish, yogurt, salad, or dried form [3,4]. In addition, it can be used to

manufacture perfumes, soaps, cosmetics, and tooth-cleaning products. It is reported that *O. basilicum* L. may be traditionally helpful in treating some diseases such as fever, headache, kidney problems, ulcers, rheumatoid arthritis, and irregular cycles in folk medicine [5]. Also, recent research showed that this plant is a potent antioxidant [6], antiviral [7], and anti-proliferative [8]. There are secondary metabolites such as essential oil, tannins, phenols, flavonoids, anthocyanins, and steroids in the chemical composition of Basil. Also, it contains fat, protein, water, minerals (especially high magnesium, potassium, and iron), and vitamins (especially choline, vitamin C, vitamin E, and vitamin K) [3].

It has been reported that, recently, many medicinal plants used in phytopharmaceutical production have been overexploited and have been exposed to microbial contaminants in their natural habitat [9]. Hence, some biotechnological methods such as callus induction and culture, micropropagation, somatic embryogenesis, and protoplast isolation and culture have been developed to culture plant cells and tissues. [4]. It provides alternatives for propagating valuable and endangered medicinal plants and allows in vitro production of secondary metabolites. Micropropagation is one of the most efficient ways to propagate plants and may significantly increase the production of secondary metabolites. In this way, some selected plant genotypes can be uniform, including in large-scale production [10]. Numerous endangered medicinal and aromatic plant species can be grown using micropropagation regardless of seasonal and climatic conditions [11]. Micropropagation is also used to analyze blooming (by accelerating production) and optimize commercial production to determine the amount of volatile compounds in plant species at different developmental stages [12]. Solid culture media consisting of Murashige-Skoog salts 3% (w/v) sucrose and benzyl adenine (B.A.) are commonly used as growth regulators in micropropagation [4].

Drying is an important stage in many processes used to obtain valuable components from *O. basilicum* L., its dry consumption, and marketing [4]. Due to reducing the water activity in the drying, the microbial growth and the chemical reactions are stopped. However, the drying method and conditions should be chosen appropriately according to the material to be dried. Various drying methods include the sun, convective hot air, microwave, infrared, and freeze. These methods have advantages and disadvantages depending on the process economy (for example, initial investment, operating costs, and energy consumption), environmental contamination, weather uncertainties, and final product quality [13]. Convective hot air dryers are commonly used to dry

food and agricultural products because they are independent of weather variations, shortened drying cycles, low nutritional loss, and improved hygiene [14]. Introducing drying kinetics, drying behavior, and energy efficiency is useful in designing the industrial dryer for drying materials. Thus, thin-layer drying models are commonly used to determine drying kinetics and to predict drying behavior and appropriate drying conditions of foods [15,16].

Özcan *et al.* [17] investigated the drying of *O. basilicum* L. using sun and oven drying methods. They found that oven drying is better than sun drying because of the dried product's shorter drying time and good mineral content. Telsfer and Galindo [18] reported that pre-treatment before *O. basilicum* L. drying shortened the drying times by 57% for air drying, 33% for vacuum drying, and 25% for freeze drying. Altay *et al.* [13] determined the drying rate, kinetics, and energy efficiency of *O. basilicum* L. leaves using the sun, freeze, hot air convective, and microwave oven. They indicated that the energy efficiency of hot air convective drying is better than that of freeze drying.

In this paper, modeling of thin layer hot air drying of micropropagated *O. basilicum* L. was statistically carried out using common-known equations. Furthermore, unlike many studies, the derived model equations, simultaneous temperature and time functions, were also used in statistical modeling tests. Finally, this work presents some quality test results of dried *O. basilicum* L. samples and an energy efficiency analysis of the drying process.

MATERIALS AND METHODS

Micropropagation of *O. basilicum* L.

O. basilicum L. seeds were planted in pots for cultivation. Then, grown seedlings were used in micropropagation experiments [19]. *O. basilicum* L. was micropropagated at the plant tissue culture laboratory of the Bioengineering Department of Firat University (Elazığ in Turkey). The micropropagation process was performed in a Murashige and Skoog (M.S.) medium with a plant growth regulator (PGR) of 0.5 mg/L Kinetin, 0.5 mg/L 2,4-dichlorophenoxyacetic acid, and 0.8% (w/v) plant agar [20]. Seedling stems were collected using a sterile scalpel. They were washed with tap water and soaked in 70% ethanol for 30 seconds before being cultured. Plant explants filtered through ethyl alcohol were alcoholized and moved into a cabinet. They were kept for 5 min in sodium hypochlorite (NaClO) diluted with 50% (v/v) distilled water. Commercial bleach (5%, v/v) was used as sodium hypochlorite. Tween agent (1 drop–2 drops) was added to the plant explants to increase the surface

contact of sodium hypochlorite. The stems of different lengths (1.5 cm–2 cm) were transferred to media containing PGR. The shoots were incubated on rooting media at 3000 lux light for 16 hours and in the dark for eight hours at $(24 \pm 1)^\circ\text{C}$ every day for four weeks. The rooted plants were gradually adapted to planting and environmental conditions during acclimatization (the final stage of micropropagation). The plants were removed from the rooting media and washed in tap water to purify them from the medium. Peat was used as a planting medium. The peat was sterilized in an autoclave at 121°C for 15 minutes. Perlite (1:1 ratio) was added to the peat and put into pots. The rooted plants were planted into those pots.

Tray dryer experiments

Tray dryer experiments were carried out in the test setup consisting of a serpentine heater, a fan, a balance, and a computer at the laboratory of the Bioengineering Department of Firat University [19]. The initial moisture content of the samples was measured using an infrared dryer (Schimadzu MOC63u, Kyoto, Japan). Each experiment involved five grams of *O. basilicum* L. leaf. The experimental studies were performed at 1 m/s air velocity and 30°C , 40°C , and 50°C . The weight of the *O. basilicum* L. samples was measured at 10 minute intervals until the difference between the two values was 0.5%. Time-dependent dry basis moisture contents (w , g moisture/g dry matter)

were calculated based on experimental data. The moisture ratio (Eq. 1) was calculated using the moisture and equilibrium moisture content [21,22]:

$$MR = \frac{w - w_e}{w_0 - w_e} \quad (1)$$

where MR is the dimensionless moisture ratio, w is the moisture content (db) at any time, w_e is the equilibrium moisture content, and w_0 is the initial solid moisture content. If the relative humidity of the drying air continuously changes, then the equilibrium moisture content measurement is difficult. In such cases, Eq. 1 can be simplified to the following equation [23,24]:

$$MR = \frac{w}{w_0} \quad (2)$$

Modeling

The experimental drying data were supplied from a previous article [19]. The moisture ratios were calculated using Eq. 2 and were statistically compared with the model equations (Table 1). The statistical analyses used nonlinear regression and a quasi-Newton optimization routine for parameter estimation (Statistica v.10). Chi-square (χ^2), the root mean square ($RMSE$), the mean squared error (RSS), and Akaike information criteria (AIC) were used to test the model fit statistically in addition to the correlation coefficient (R).

Table 1. Mathematical models used to compare the experimental moisture ratio of *O. basilicum* L. samples statistically.

Model no	Model names	Mathematical expressions	References
1	Newton	$MR = \exp(-kt)$	[25]
2	Page	$MR = \exp(-kt^n)$	[26]
3	Henderson and Pabis	$MR = a \exp(-kt)$	[27]
4	Logarithmic	$MR = a \exp(-kt) + c$	[28]
5	Wang and Singh	$MR = 1 + at + bt^2$	[29]
6	Diffusion	$MR = a \exp(-kt) + (1-a) \exp(-kbt)$	[30]
7	Verma	$MR = a \exp(-kt) + (1-a) \exp(-gt)$	[31]
8	Two-term exponential	$MR = a \exp(-kt) + (1-a) \exp(-kat)$	[32]

$$\chi^2 = \frac{\left(\sum_{i=1}^N (MR_{\text{exp},i} - MR_{\text{pred},i})^2 \right)}{N - n} \quad (3)$$

$$RMSE = \left[\left(\frac{1}{2} \sum_{i=1}^N (MR_{\text{exp},i} - MR_{\text{pred},i})^2 \right) \right]^{0.5} \quad (4)$$

$$RSS = \sum_{i=1}^N (MR_{\text{exp},i} - MR_{\text{pred},i})^2 \quad (5)$$

$$AIC = -2 \ln L + 2p \quad (6)$$

where $MR_{\text{exp},i}$ and $MR_{\text{pred},i}$ are the experimental and calculated moisture ratios, respectively, N is the

number of data used in calculations, and n is the number of constants in model equations. In Eq. (6), L and p are the model equations' maximum likelihood and number of parameters [33]. The closer the chi-square (χ^2) or AIC, which is more useful when low data numbers are to zero, the better the fit between experimental and calculated data [34].

Quality tests

In this section, some chemical and physical properties of dried *O. basilicum* L. samples were

determined. For this purpose, total phenolic content, total flavonoid content, and antioxidant capacity values were measured, and the results were reported as means \pm standard deviation for triplicate determinations. Also, FTIR and SEM analyses of dried *O. basilicum* L. samples were carried out.

Total phenolic content analysis

The phenolic content was measured using the Folin-Ciocalteu method [35]. According to this method, 300 μ l of *O. basilicum* L. callus extract and 1.5 ml of 2 N Folin-Ciocalteu reagent were mixed in glass tubes. After this mixture was left for (1–2) minutes, 1.2 ml of 7.5% sodium carbonate solution was added, mixed in a vortex, and kept in the dark at 25 °C for 90 minutes. Its absorbance was measured at 765 nm against a blank (pure water) in a UV-VIS spectrophotometer (Shimadzu UV-mini-1240, Kyoto, Japan). Total phenol content was given as gallic acid equivalent (GAE) using the gallic acid calibration curve.

Total flavonoid analysis

The methanolic form was used to analyze the total flavonoid content [36]. For this analysis, 1 ml of plant callus extract and 1 ml of 2% $AlCl_3$ solution were mixed. The mixture was kept at room temperature (25 °C) for 10 minutes. The absorbances of the samples were read in a UV-VIS spectrophotometer (Shimadzu UV-mini-1240, Kyoto, Japan) at a wavelength of 394 nm against 2% $AlCl_3$ as a control sample. The flavonoid concentration was calculated by comparing it with the calibration curve of quercetin.

Antioxidant capacity analysis

Dried *O. basilicum* L. samples were subjected to methanol extraction at the solid/solvent ratio of 1:10 (g/mL) using a homogenizer to gain antioxidants in its content. Then, the extract obtained was centrifuged at 7000 rpm for ten minutes. The supernatant was used to determine antioxidant capacity using two common methods (ABTS and DPPH).

ABTS scavenging capacity

The antioxidant capacity of *O. basilicum* L. extracts was measured based on ABTS's radical cation scavenging ability [2,2'- azonobis(3- ethylbenzothiazoli ne-6-sulfonate)]. At the time of analysis, 1900 μ l of diluted ABTS solution and 100 μ l of *O. basilicum* L. callus extracts were added to the glass tubes and mixed in a dark room for 1 h. The absorbance of these mixtures was read against a blank (phosphate buffer) in a UV-VIS spectrophotometer (Shimadzu UV-mini-1240, Kyoto, Japan) at 734 nm. The inhibition percent

of the ABTS was calculated using the following equation [37,38]. Also, the antioxidant capacity was given as Trolox equivalents antioxidant capacity (mmol TEAC/100 g dry *O. basilicum* L.).

$$ABTS \text{ inhibition}(\%) = \left(\frac{A_{Control} - A_{Sample}}{A_{Control}} \right) \times 100 \quad (7)$$

DPPH scavenging capacity

The antioxidant capacity was also measured using DPPH [α -Diphenyl-b-picrylhydrazyl] method. For this purpose, DPPH solution (25 mg/L) was prepared in methanol. First, 4 ml of DPPH solution was mixed with 100 μ l of *O. basilicum* L. extracts in the test tubes. Then these mixtures were vortexed and then incubated in the dark at 25 °C for 30 minutes. Finally, the absorbance was measured against a blank (methanol) at 517 nm [39]. The inhibition percent of the DPPH was calculated using the following equation:

$$DPPH \text{ inhibition}(\%) = \left(\frac{A_{Control} - A_{Sample}}{A_{Control}} \right) \times 100 \quad (8)$$

FTIR and SEM analyses

Fourier-transform infrared (FTIR) spectroscopy of the dried *O. basilicum* L. samples was performed by Shimadzu IR Spirit Spectrophotometer QATR-S (Kyoto, Japan) device with a resolution of 4 cm^{-1} and the wave number ranging from 4.000 cm^{-1} to 400 cm^{-1} . In addition, the SEM image of the dried *O. basilicum* L. samples was observed using Carl Zeiss Evo MA10 (USA) device.

The energy efficiency of a hot-air dryer

The energy efficiency of the hot-air drying system was carried out at 1 m/s air velocity and 30 °C, 40 °C, and 50 °C. For this purpose, the specific moisture extraction rate (SMER), the moisture extraction rate (MER), and specific energy consumption (SEC) were calculated using the following Eqs. (9–11) [13]:

$$SMER = \frac{\text{Amount of water removed during drying (kg)}}{\text{Total energy supplied in drying process (kWh)}} \quad (9)$$

$$MER = \frac{\text{Amount of water removed during drying (kg)}}{\text{Drying time (h)}} \quad (10)$$

$$SEC = \frac{\text{Total energy supplied in drying process (kWh)}}{\text{Amount of water removed during drying (kg)}} \quad (11)$$

The total electrical current drawn by the hot-air dryer at a particular airspeed and drying temperature was measured with a DT3266L Clamp Multimeter Voltmeter Ammeter. The voltage, current, and time values were carried out under stable operating conditions of the dryer. As a result, the electrical power(kWh) was calculated as follows: The electrical

energy = current * voltage * time (h).

RESULTS AND DISCUSSION

Grown *O. basilicum* L. plants have soft leaves ranging from light green to dark green, 1 cm–5 cm in length and 1 cm–3 cm in width.

Modeling results based on drying time-dependent equations

The model constants and some statistical parameters of the eight equations used to model the drying of *O. basilicum* L. are given in Table 2. Verma equation (model 4) best fits the experimental moisture ratios at all temperatures. This result is based on having

the lowest Chi-square (χ^2) and AIC values [13,23,34]. Page equation (model 2) provided the second-best fit between the experimental and predicted moisture ratios. Altay *et al.* [13] produced *O. basilicum* L. using conventional methods and then examined the thin-layer drying of leaves. They found that the modified Henderson and Pabis, logarithmic, and Page equations best represented the sun, freezing, and microwave-convective drying, respectively. This study also employed convective drying. Altay *et al.* [13] did not test the Verma equation. We found that the Page was one of the equations that provided the best fit in drying *O. basilicum* L., which was micropropagated based on modeling. This result is consistent with that of Altay *et al.*

Table 2. The value of constants in model equations and some statistical parameters obtained from statistical analyses for drying *O. basilicum* L. samples at 1 m/s flow rate and different temperatures.

Model No	k	n	a	b	c	g	RMSE	RSS	χ^2	AIC
30 °C										
1	0.0047	-	-	-	-	-	0.0913	0.0167	1.915x10 ⁻⁴	-742.775
2	0.0045	1.0106	-	-	-	-	0.0906	0.0164	1.910x10 ⁻⁴	-742.007
3	0.0046	-	0.9813	-	-	-	0.0854	0.0146	1.695x10 ⁻⁴	-176.024
4	Not suitable	-	-	-	-	-	-	-	-	-
5	-	-	-0.0031	2.360x10 ⁻⁶	-	-	0.3660	0.2679	3.115x10 ⁻³	-499.137
6	Not suitable	-	-	-	-	-	-	-	-	-
7	1.6276	-	0.0225	-	-	0.0046	0.0841	0.0141	1.665x10 ⁻⁴	-752.985
8	Not suitable	-	-	-	-	-	-	-	-	-
40 °C										
1	0.0132	-	-	-	-	-	0.0869	0.0151	1.738x10 ⁻⁴	-751.233
2	0.0071	1.1359	-	-	-	-	0.0406	0.0033	3.827x10 ⁻⁵	-881.877
3	0.0137	-	1.0348	-	-	-	0.0779	0.0121	1.409x10 ⁻⁴	-768.445
4	0.0134	-	1.0369	-	-0.0055	-	0.0717	0.0103	1.195x10 ⁻⁴	-780.797
5	Not suitable -	-	-	-	-	-	-	-	-	-294.900
6	Not suitable	-	-	-	-	-	-	-	-	-
7	0.0210	-	-6.8356	-	-	0.0196	0.0345	0.0024	2.806x10 ⁻⁵	-907.868
8	4.0043	-	0.0033	-	-	-	0.0886	0.0157	1.826x10 ⁻⁴	-743.904
50 °C										
1	0.0237	-	-	-	-	-	0.0233	0.0011	1.246x10 ⁻⁵	-980.465
2	0.0211	1.0291	-	-	-	-	0.0193	0.0007	8.646x10 ⁻⁶	-1011.28
3	0.0238	-	1.0060	-	-	-	0.0227	0.0010	1.193x10 ⁻⁵	-983.267
4	0.0237	-	1.0065	-	-0.0013	-	0.0212	0.0009	1.048x10 ⁻⁵	-992.577
5	Not suitable -	-	-	-	-	-	-	-	-	-
6	0.0319	-	-1.0409	0.858069	-	-	0.0178	0.0006	7.489x10 ⁻⁶	-1022.80
7	0.0302	-	-3.4147	-	-	0.0285	0.0177	0.0006	7.389x10 ⁻⁶	-1023.97
8	Not suitable	-	-	-	-	-	-	-	-	-

Figure 1 presents a graph showing the changes in experimental and predicted moisture ratios for the studied models, except for three model equations (Logarithmic, Diffusion, and Two-term exponential) where there is no fit. As seen from Figure 1, Wang and Singh's model amongst studied model equations is a poor fit. But, the fit of four model equations (Newton, Page, Henderson and Pabis, and Verma) is good since the actual and calculated values are on the diagonal. The following equations are time-dependent moisture ratio equations based on the modeling performed using the Verma equation with the highest fit at 30 °C, 40 °C, and 50 °C:

$$MR = 0.0225 \exp(-1.6276t) + 0.9775 \exp(-0.0046t), \quad (12)$$

at 30°C

$$MR = 0.0210 \exp(-6.8356t) + 0.9790 \exp(-0.0196t), \quad (13)$$

at 40°C

$$MR = 0.0302 \exp(-3.4147t) + 0.9698 \exp(-0.0285t), \quad (14)$$

at 50°C

Modeling drying curves using derived models

It is also possible to perform advanced modeling with the thin layer models by expressing the constants in the equations as a function of temperature [40]. The Verma and Page equations were the most suitable models for drying *O. basilicum* L. Table 3 shows the derived Verma and Page model equations defined according to exponent and exponential type

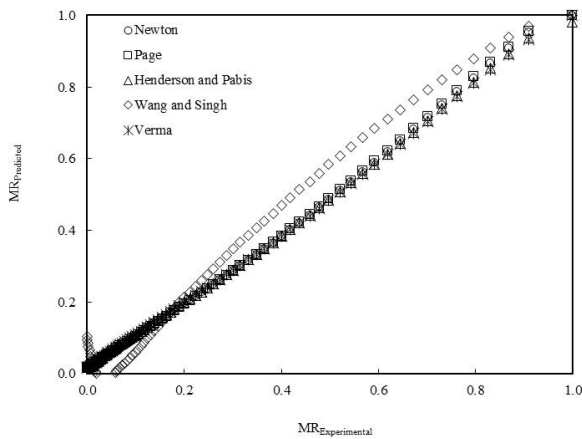


Figure 1. Changing the experimental moisture ratio with the predicted moisture ratio obtained from models used at an air velocity of 1 m/s and 30 °C.

expressions (Eq. 15 and Eq.16).

$$\text{Exponent type} = aT^b \tag{15}$$

$$\text{Exponent type} = a \exp(bT) \tag{16}$$

Table 4 shows the model constants and some statistical parameters obtained from the statistical analyses with derived model equations for drying *O. basilicum* L. As can be seen in Table 4, Eq. D9 is the model equation having the lowest RMSE, MSE, χ^2 , and AIC.

D9 is obtained from the Verma model, and all its constants exponentially depend on temperature. For *O. basilicum* L. drying, the dependence of the moisture ratio (M.R.) on the temperature and the drying time is given in the following equation:

Table 3. Derived model equations obtained from Page and Verma models [40].

Model No	Source model	Mathematical expressions
D1	Page model	$MR = \exp(-k_1 T^{k_2} t)^{n_1 \exp(n_2 T)}$
D2		$MR = \exp(-k_1 T^{k_2} t)^{n_1 T^{n_2}}$
D3		$MR = \exp(-k_1 \exp(k_2 T) t)^{n_1 \exp(n_2 T)}$
D4		$MR = \exp(-k_1 \exp(k_2 T) t)^{n_1 T^{n_2}}$
D5	Verma model	$MR = a_1 T^{a_2} \exp(-k_1 T^{k_2} t) + (1 - a_1 T^{a_2}) \exp(-g_1 \exp(g_2 T) t)$
D6		$MR = (a_1 \exp(a_2 T)) \exp(-k_1 T^{k_2} t) + (1 - a_1 \exp(a_2 T)) \exp(-g_1 \exp(g_2 T) t)$
D7		$MR = a_1 T^{a_2} \exp(-k_1 \exp(k_2 T) t) + (1 - a_1 T^{a_2}) \exp(-g_1 \exp(g_2 T) t)$
D8		$MR = (a_1 \exp(a_2 T)) \exp(-k_1 \exp(k_2 T) t) + (1 - a_1 \exp(a_2 T)) \exp(-g_1 T^{g_2} t)$
D9		$MR = (a_1 \exp(a_2 T)) \exp(-k_1 \exp(k_2 T) t) + (1 - a_1 \exp(a_2 T)) \exp(-g_1 \exp(g_2 T) t)$

Table 4. The value of model constants in derived model equations and some statistical parameters obtained from statistical analyses for drying of micropropagated *O. basilicum* L. samples.

Model No	k ₁	k ₂	n ₁	n ₂	a ₁	a ₂	g ₁	g ₂	RMSE	RSS	χ^2	AIC
D1	0.0043	0.1950	0.6045	-0.0004	-	-	-	-	1.1797	2.7835	0.0208	-525.791
D2	0.0100	0.0052	0.6349	0.0000	-	-	-	-	1.4165	4.0130	0.0299	-475.669
D3	0.1588	-0.0859	10.9700	-0.0801	-	-	-	-	2.1466	9.2159	0.0688	-361.770
D4	0.0118	-0.0011	0.7906	0.00001	-	-	-	-	1.4101	3.9770	0.0216	-476.904
D5	0.1015	0.0000	-	-	0.1294	0.2599	0.0049	-0.0009	1.1882	2.8237	0.0214	-519.826
D6	-0.0099	0.1366	-	-	0.9537	-0.0284	0.0289	0.1863	1.1788	2.7792	0.0210	-521.999
D7	-0.8269	-0.6509	-	-	0.0520	0.0000	0.0134	-0.0012	1.1882	2.8238	0.0155	-519.822
D8	0.2185	0.1400	-	-	0.8811	-0.5139	0.0088	0.0000	1.2931	3.3441	0.0184	-496.650
D9	0.0099	0.0154	-	-	0.1447	0.0204	0.0107	0.0109	1.1532	2.6597	0.0146	-528.022

$$MR = (0.1447 \exp(0.0204T)) \exp(-(0.0099 \exp(0.0154T))t) + (1 - 0.1447 \exp(0.0204T)) \exp(-(0.0107 \exp(0.0167T))t) \tag{17}$$

Eq. 17 was obtained using D9, best representing the drying phenomenon among the derived models. The change of experimental and predicted according to Eq. 17 moisture ratios with drying time was illustrated in Figure 2. As shown in Figure 2, the developed model at 40 °C and 50 °C is better than at 30 °C. It indicates that the derived models are more effective at higher drying temperatures.

Quality test results

The total phenolic and flavonoid contents of micropropagated *O. basilicum* L. samples were measured as (2.538 ± 0.029) mg GAE/g, and (2.017 ± 0.088) mg quercetin/g, respectively. Mahirah *et al.* [41] determined the total phenolic content of *O. basilicum* L. as 2.61 mg GAE/g. In the literature, it has been shown that the flavonoid content of *O. basilicum* L. varies between 0.7 mg quercetin/g and 4.97 mg quercetin/g [42,43]. ABTS and DPPH inhibition (%) values of dried *O. basilicum* L. sample obtained using the micropropagation technique were 91.44 ± 0.419 and 95.528 ± 0.128 at 40 °C,

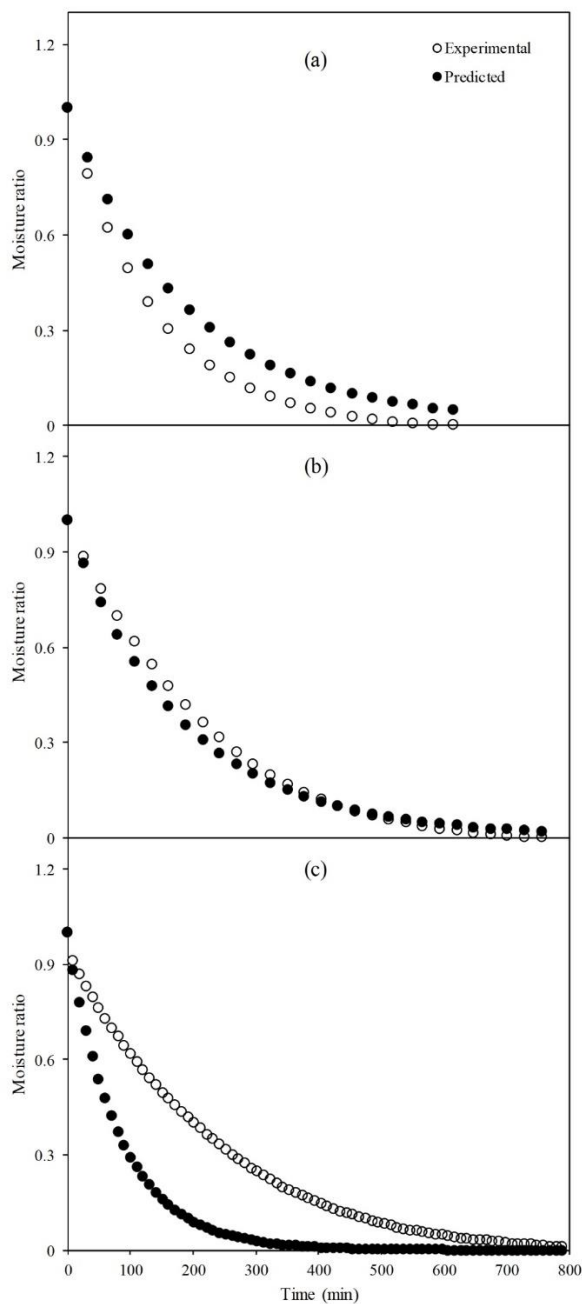
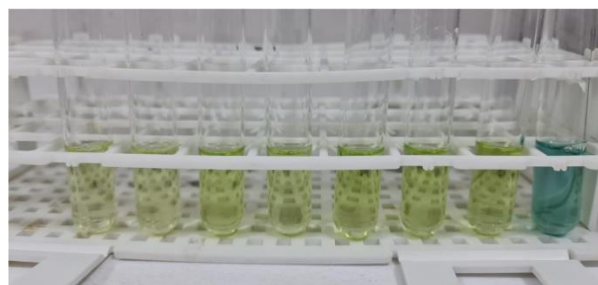


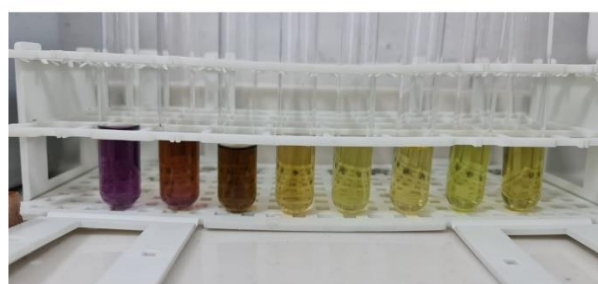
Figure 2. Change of the experimental and calculated (using Eq. 17) moisture ratios with the drying time for drying of *O. basilicum* L. at (a) 50 °C, (b) 40 °C, and (c) 30 °C.

respectively. In this context, the pictures supplied from ABTS and DPPH inhibition (%) experiments carried out using different *O. basilicum* L. extracts were illustrated in Figure 3. It was found that the inhibition (%) values calculated from both ABTS and DPPH methods were close to each other. Also, the antioxidant capacity of *O. basilicum* L. was calculated at (2.263 ± 0.001) mmol TEAC/100 g d.w. Kwee and Niemeyer [44] measured the antioxidant capacities of 15 basil (*O. basilicum* L.) cultivars. They determined that these capacity values varied from

0.28 mmol/100 g d.w. to 11.5 mmol/100 g d.w. Therefore, the antioxidant capacity of micropropagated *O. basilicum* L. grown agrees with the literature.



(a)



(b)

Figure 3. The color change of (a) ABTS and (b) DPPH solutions with the addition of *O. basilicum* L. extracts at different concentrations.

The FTIR spectra of *O. basilicum* L. samples are illustrated in Figure 4 at the temperature range of 30 °C to 50 °C. As seen in Figure 4, the spectrum peaks were observed in the same wavelength values at all temperatures studied. So, it can be said that no structural decomposition occurred during the drying of the basil samples. It has been observed that alkanes with C-H rock bond and C-H stretch, aromatics with C-C stretch, and amines/amides with N-H stretch are found in the wavelength ranges of 1350 cm^{-1} – 1370 cm^{-1} , 2850 cm^{-1} – 3000 cm^{-1} , 1585 cm^{-1} – 1600 cm^{-1} , 3250 cm^{-1} – 3400 cm^{-1} , respectively. These wavelength ranges were supplied from a previous study using *O. basilicum* crude powder [45].

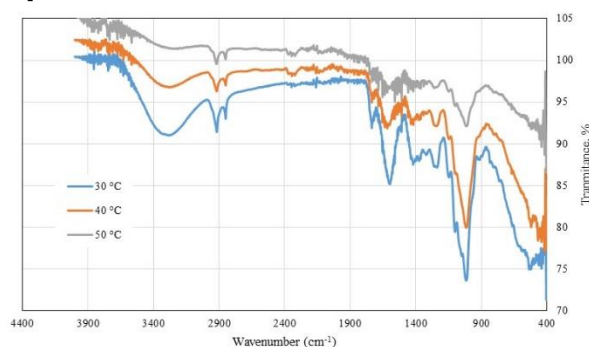


Figure 4. FTIR spectra of micropropagated *O. basilicum* L. samples in the temperature range of 30 °C to 50 °C.

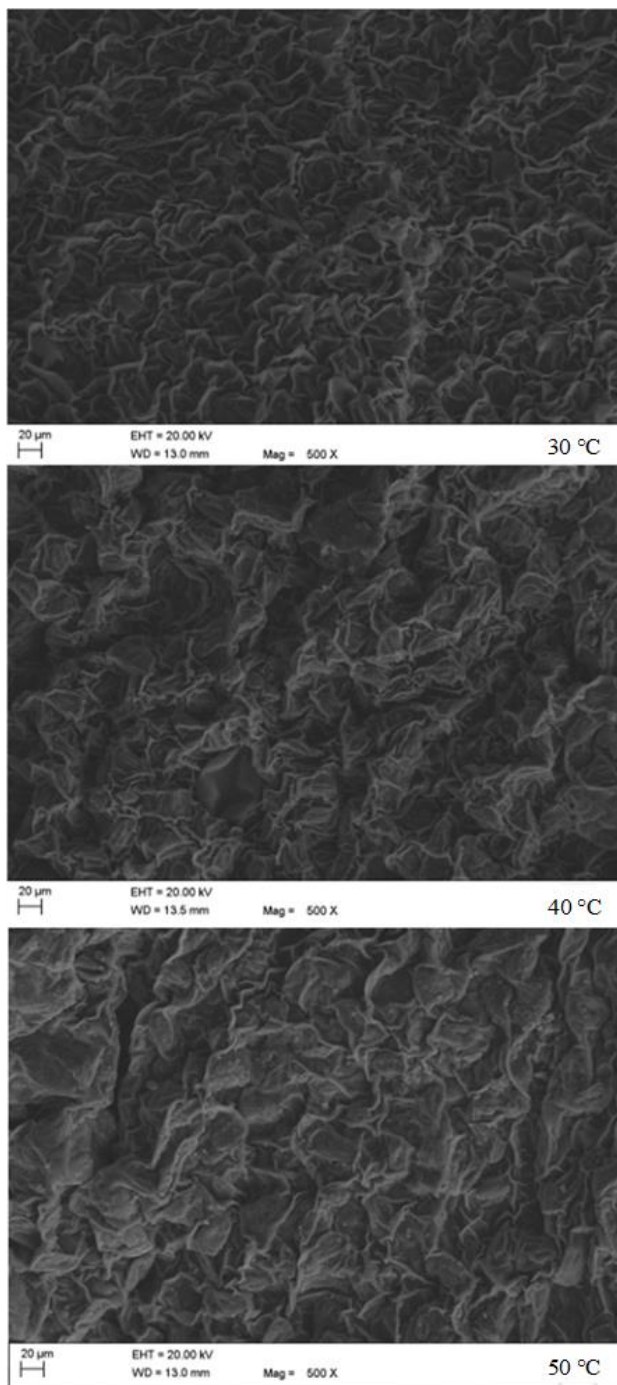


Figure 5. SEM images of micropropagated *O. basilicum L.* samples in the temperature range of 30°C to 50 °C.

The SEM images of dried *O. basilicum L.* are shown in Figure 5 at different drying temperatures. It is apparent that there are changes on the basil leaves' surface with the drying temperature. A collapse in the leaf's surface has been clearly observed at high temperatures. Similar results were obtained in the previous studies on basil or other plants [18,46,47]. However, FTIR results showed that these changes almost do not affect the functional groups on the surface of the *O. basilicum L.* leaves.

Energy efficiency results

The energy consumption values (SMER, MER, and SEC) of the hot-air dryer used in the micropropagated *O. basilicum L.* drying are given in Table 5. Table 5 shows that the energy consumed by the hot-air drying system used to dry the micropropagated *O. basilicum L.* increased with the drying temperature.

Table 5. The energy efficiency results of micropropagated *O. basilicum L.* at the 1 m/s air velocity at the studied temperatures.

Temperature (°C)	SMER (kg/kWh)	MER (kg/h)	SEC (kWh/kg)
30	0.0026	0.0003	387.67
40	0.0043	0.0007	234.81
50	0.0033	0.0011	306.61

A similar result for the energy consumption studies of tomato slices drying was obtained [48]. As seen in Table 5, the highest SMER and the lowest SEC values for drying the basil samples were obtained at 40 °C. The higher the SMER value, the better the drying efficiency. On the contrary, low SEC values are desired in the drying processes [13]. Although the energy consumption at 40 °C is lower than at 30 °C, the drying time at 40 °C (4.9 h) is clearly lower than at 30 °C (14.5 h). The electrical power (kW) of a hot air-drying system is multiplied by the drying time (h) to obtain the total energy consumption in SMER and SEC equations (Eq. 9 and Eq.11) [49].

Thus, it was determined that while the SMER value of the drying system at 40 °C is greater than at 30 °C, the SEC value is lower. However, while the SMER value at 50 °C is lower than at 40 °C, the SEC value is greater. It can be considered that this may be due to close drying times at these two temperatures (40 °C and 50 °C) and the higher energy consumption at 50 °C. Pal *et al.* [50] and Mancuhan *et al.* [51] obtained similar results in their studies on the changes in SMER and SEC values with the drying temperature.

As expected, the MER (the amount of water removed in unit time) for drying micropropagated *O. basilicum L.* drying increases with increasing temperature [13]. The SMER and SEC results clearly show that the drying time affected energy consumption. This result is in agreement with that of a previous study [52]. As a result, it can be said that the best drying condition of micropropagated *O. basilicum L.* at 1 m/s air velocity is 40 °C. As seen in Table 6, the SMER value obtained from the present study agrees with previous studies using convective drying.

Table 6. The comparison of SMER values of this study with previous studies at different drying techniques.

Plant	Drying methods	Drying conditions	SMER (kg/kWh)	References
Orange slices	Convective	50 °C, machine learning	0.0040	[53]
Apple slices	Convective	50 °C	0.0500	[54]
Apple slices	Microwave	360 W	0.5800	[54]
Apple slices	Freeze	-56 °C, 100 kPa	0.0100	[54]
<i>O. basilicum</i> L.*	Microwave	350 W	0.3340	[13]
<i>O. basilicum</i> L.*	Freeze	-48 °C, 13.33 Pa	0.0010	[13]
<i>O. basilicum</i> L.*	Convective	55 °C, 1.5 m/s	0.0080	[13]
<i>O. basilicum</i> L.*	Convective	50 °C, 1.5 m/s	0.0080	[13]
<i>O. basilicum</i> L.*	Convective	45 °C, 1.5 m/s	0.0120	[13]
<i>O. basilicum</i> L.**	Convective	40 °C, 1.5 m/s	0.0043	This study

*grown as conventional; **micropropagated

CONCLUSION

Among the eight drying model equations used in the statistical tests, Verma and Page models having low χ^2 and AIC described efficiently the hot air thin layer drying of *O. basilicum* L. leaves at all temperatures studied. The statistical analyses performed using the derived models obtained from Verma and Page models indicated that the best-representing model was D9 based on the Verma equation. The total phenolic content, total flavonoid content, and antioxidant capacity of *O. basilicum* L. samples were measured as 2.538 ± 0.029 mg GAE/g, 2.017 ± 0.088 mg quercetin/g, and 2.263 ± 0.001 mmol TEAC/100 g d.w., respectively. These characteristic values of the basil sample agreed with those of previous studies in the literature. From FTIR spectra, it has been observed that *O. basilicum* L. samples contain alkanes (C-H rock bond and C-H stretch), aromatics (C-C stretch), and amines/amides (N-H stretch). The bonds and stretching frequencies in the FTIR spectra of dried *O. basilicum* L. samples were typical at all studied temperatures. SEM images showed a collapse on the surface of *O. basilicum* L. leaves at exceptionally high temperatures. But, it can be said that this change does not affect functional groups on the surface of the *O. basilicum* L. leaves. The energy efficiency results determined an optimum temperature point (40 °C) in the SMER, and SEC values change with the drying temperature. As expected, MER values of the drying of the basil leave samples are increasing with the increasing temperature. In future studies, thin-layer drying behavior, final product quality, and energy efficiency of the dryer can be investigated for *O. basilicum* L. grown using different tissue culture techniques.

REFERENCES

- [1] J.E. Simon, M.R. Morales, W.B. Phippen, R.F. Vieira, Z. Hao, Basil: A source of aroma compounds and a popular culinary and ornamental herb, Janick J (Ed) ASHS press, Alexandria, VA, (1999), p 499.
- [2] K. Carović-Stanko, Z. Liber, V. Besendorfer, B. Javornik, B. Bohanec, I. Kolak, Z. Satovic, Plant Sys Evol Suppl 285 (2010) 13–22. <https://doi.org/10.1007/s00606-009-0251-z>.
- [3] S. Filip, Int. J. Clin. Nutr. Diet 3 (2017) 118. <https://doi.org/10.15344/2456-8171/2017/118>.
- [4] O. Makri, S. Kintzios, J. Herbs, Spices Med. Plants 13 (2008) 123–150. https://doi.org/10.1300/J044v13n03_10.
- [5] K. Dhama, K. Sharun, M.B. Gugjoo, R. Tiwari, M. Alagawany, M. Iqbal Yattoo, P. Thakur, H.M. Iqbal, W. Chaicumpa, I. Michalak, Food Rev. Int. (2021) 1–29. <https://doi.org/10.1080/87559129.2021.1900230>.
- [6] C. Jayasinghe, N. Gotoh, T. Aoki, S. Wada, J. Agric. Food Chem. 51 (2003) 4442–4449. <https://doi.org/10.1021/jf034269o>.
- [7] L.C. Chiang, L.T. Ng, P.W. Cheng, W. Chiang, C.C. Lin, Clin. Exp. Pharmacol. Physiol. 32 (2005) 811–816. <https://doi.org/10.1111/j.1440-1681.2005.04270.x>.
- [8] A.B. Mohammed, S. Yagi, T. Tzanova, H. Schohn, H. Abdelgadir, A. Stefanucci, A. Mollica, M.F. Mahmoodally, T.A. Adlan, G. Zengin, S. Afr. J. Bot. 132 (2020) 403–409. <https://doi.org/10.1016/j.sajb.2020.06.006>.
- [9] A. Aye, Y.-D. Jeon, J.-H. Lee, K.-S. Bang, J.-S. Jin, Oriental Pharmacy and Experimental Medicine 19 (2019) 217–226. <https://doi.org/10.1007/s13596-019-00372-2>.
- [10] N.A. Arikat, F.M. Jawad, N.S. Karam, R.A. Shibli, Sci. Hortic. (Amsterdam, Neth.) 100 (2004) 193–202. <https://doi.org/10.1016/j.scienta.2003.07.006>.
- [11] R.L.M. Pierik, In vitro culture of higher plants, Kluwer Academic Publisher, Boston, (1997), p.301. 0792345274.
- [12] M. Debnath, C. Malik, P.S. Bisen, Curr. Pharm. Biotechnol. 7 (2006) 33–49. DOI: 10.2174/138920106775789638.
- [13] K. Altay, A.A. Hayaloglu, S.N. Dirim, Heat Mass Transfer. 55 (2019) 2173–2184. <https://doi.org/10.1007/s00231-019-02570-9>.
- [14] S. Fang, Z. Wang, X. Hu, Int. J. Food Sci. Technol. 44 (2009) 1818–1824. <https://doi.org/10.1111/j.1365-2621.2009.02005.x>.
- [15] B. Tepe, T.K. Tepe, A. Ekinçi, Chem. Ind. Chem. Eng. Q. 22 (2022) 151–159. <https://doi.org/10.2298/CICEQ210126026T>.
- [16] A.C. Ersan, N. Tugrul, Chem. Ind. Chem. Eng. Q. 27 (2021) 319–328. <https://doi.org/10.2298/CICEQ201114050E>.
- [17] M. Özcan, D. Arslan, A. Ünver, J. Food Eng. 69 (2005) 375–379. <https://doi.org/10.1016/j.jfoodeng.2004.08.030>.
- [18] A. Telfser, F.G. Galindo, LWT 99 (2019) 148–155. <https://doi.org/10.1016/j.lwt.2018.09.062>.
- [19] A. Topdemir, J. Firat Univ. Eng. Sci. 31 (2019) 545–550. <https://doi.org/10.35234/fumbd.580212>.
- [20] T. Murashige, F. Skoog, Physiol. Plant. 15 (1962) 473–497. <https://doi.org/10.1111/j.1399-3054.1962.tb08052.x>.
- [21] C.J. Geankoplis, A.A. Hersel, D.H. Lepek, Transport processes and separation process principles, Prentice Hall Boston, (2018). ISBN 0-13-045253-X.
- [22] J.M. Coulson, J.F. Richardson, J.R. Backhurst, J.H. Harker, Chemical Engineering: Fluid flow, heat transfer and mass transfer, Pergamon press, London, (1954). ISBN: 9788181473868.
- [23] Z. Erbay, F. Icier, Crit. Rev. Food Sci. Nutr. 50 (2010) 441–

464. <https://doi.org/10.1080/10408390802437063>.
- [24] C. Ertekin, M.Z. Firat, Crit. Rev. Food Sci. Nutr. 57 (2017) 701–717. <https://doi.org/10.1080/10408398.2014.910493>.
- [25] Q. Liu, F. Bakker-Arkema, J. Agric. Eng. Res. 66 (1997) 275–280. <https://doi.org/10.1006/jaer.1996.0145>.
- [26] G.E. Page, Factors Influencing the Maximum Rates of Air Drying Shelled Corn in Thin layers., Master Thesis, Purdue University(1949). 1083231995.
- [27] S. Henderson, S. Pabis, J. Agric. Eng. Res. 7 (1962) 85–89.
- [28] A. Yağcıoğlu, A. Değirmencioğlu, F. Çağatay, Drying characteristics of laurel leaves under different drying conditions, in 7th Int Congr. Agric. Mechan. Energy, (1999) 565–569.
- [29] C. Wang, R. Singh, Trans. Am. Soc. Agric. Eng. 11 (1978) 668–672.
- [30] A. Kassem, Comparative studies on thin layer drying models for wheat, 13th Int. Congr. Agric. Eng., (1998) 2–6.
- [31] M. Kalender, Constr. Build. Mater. 155 (2017) 947–955. <https://doi.org/10.1016/j.conbuildmat.2017.08.094>.
- [32] L. Bennamoun, L. Kahleras, F. Michel, L. Courard, T. Salmon, L. Fraikin, A. Belhamri, A. Léonard, Int. J. Energy Eng. 3 (2013) 1–6. <https://hdl.handle.net/2268/134220>.
- [33] H. Akaike, Factor analysis and AIC, Springer, New York, (1987). ISBN 0-387-98355-4.
- [34] F.P. Gomes, R. Osvaldo, E.P. Sousa, D.E. de Oliveira, F.R.d. Araújo Neto, Revista Brasileira de Engenharia Agrícola e Ambiental 22 (2018) 499–505. <https://doi.org/10.1590/1807-1929/agriambi.v22n12p866-871>.
- [35] V.L. Singleton, J.A. Rossi, Am. J. Enol. Vitic. 16 (1965) 144–158. DOI: 10.5344/ajev.1965.16.3.144.
- [36] J. Lamaison, C. Petitjean-Freytet, A. Carnat, Annales Pharmaceutiques Françaises (France) 48 (1990) 103–108.
- [37] N.J. Miller, A.T. Diplock, C.A. Rice-Evans, J. Agric. Food Chem. 43 (1995) 1794–1801. <https://doi.org/10.1021/jf00055a009>.
- [38] Y. Gökçe, H. Kanmaz, B. Er, K. Sahin, A. Hayaloglu, Food Bioscience 43 (2021) 101228. <https://doi.org/10.1016/j.fbio.2021.101228>.
- [39] W. Brand-Williams, M.-E. Cuvelier, C. Berset, LWT-Food science and Technology 28 (1995) 25–30. [https://doi.org/10.1016/S0023-6438\(95\)80008-5](https://doi.org/10.1016/S0023-6438(95)80008-5).
- [40] H. Toğrul, J. Food Eng. 77 (2006) 610–619. <https://doi.org/10.1016/j.jfoodeng.2005.07.020>.
- [41] Y. Siti Mahirah, M. Rabeta, R. Antora, Food Res. 2 (2018) 421–428. [https://doi.org/10.26656/fr.2017.2\(5\)](https://doi.org/10.26656/fr.2017.2(5)).
- [42] R. Oonsivilai, P. Prasongdee, Total phenolic contents, total flavonoids and antioxidant activity of Thai basil (*Ocimum basilicum* L.), 5th Int. Conf. Nat. Prod. Health Beauty, Thailand, (2014).
- [43] H. Abramovic, V. Abram, A. Cuk, B. Ceh, S. Smole-Mozina, M. Vidmar, M. Pavlovic, N.P. Ulrih, Turk. J. Agric. For. 42 (2018) 185–194. <https://doi.org/10.3906/tar-1711-82>.
- [44] E.M. Kwee, E.D. Niemeyer, Food Chem. 128 (2011) 1044–1050. <https://doi.org/10.1016/j.foodchem.2011.04.011>.
- [45] U. Nazir, S. Javaid, H. Awais, F. Bashir, M. Shahid, Pure Appl. Biol. 10 (2021) 1004–1013. <http://dx.doi.org/10.19045/bspab.2021.100105>.
- [46] A.N. Yousif, C.H. Scaman, T.D. Durance, B. Girard, J. Agric. Food Chem. 47 (1999) 4777–4781. <https://doi.org/10.1021/jf990484m>.
- [47] D. Argyropoulos, J. Müller, Ind. Crops Prod. 52 (2014) 118–124. <https://doi.org/10.1016/j.indcrop.2013.10.020>.
- [48] M. Dorouzi, H. Morteza pour, H.-R. Akhavan, A.G. Moghaddam, Solar Energy 162 (2018) 364–371. <https://doi.org/10.1016/j.solener.2018.01.025>.
- [49] M. Ahmadi, K.R. Gluesenkamp, S. Bigham, Energy Convers. Manage. 230 (2021) 113763. <https://doi.org/10.1016/j.enconman.2020.113763>.
- [50] U. Pal, M.K. Khan, S. Mohanty, Drying Technol. 26 (2008) 1584–1590. <https://doi.org/10.1080/07373930802467144>.
- [51] E. Mancuhan, S. Özen, P. Sayan, S.T. Sargut, Drying Technol. 34 (2016) 1535–1545. <https://doi.org/10.1080/07373937.2015.1135340>.
- [52] A. Tarafdar, N. Jothi, B.P. Kaur, J. Appl. Res. Med. Aromat. Med. Plants 24 (2021) 100306. <https://doi.org/10.1016/j.jarmap.2021.100306>.
- [53] N. Çetin, J. Food Process. Preserv. 46 (2022) e17011. <https://doi.org/10.1111/jftp.17011>.
- [54] T. Baysal, N. Ozbalta, S. Gokbulut, B. Capar, O. Tastan, G. Gurlek, Therm. Sci. Technol. 35 (2015) 135–144.

MEHMET KALENDER
AYKUT TOPDEMIR

Department of Bioengineering,
Firat University, Elazığ, Turkey

NAUČNI RAD

ISTRAŽIVANJE SUŠENJA MIKROPROPAGIRANOG *OCIMUM BASILICUM* L. U TANKOM SLOJU: MODELOVANJE, KARAKTERISTIKE KVALITETA I ENERGETSKA EFIKASNOST

*Ova studija prikazuje modelovanje sušenja mikropropagiranog *Ocimum basilicum* L. u tankom sloju, neke karakteristike kvaliteta osušenog proizvoda i analizu potrošnje energije za korišćenu sušaru. U statističkim analizama korišćeni su eksperimentalni podaci o sušenju dobijeni iz prethodnog članka. Statističko modelovanje je sprovedeno korišćenjem eksperimentalnih podataka pri brzini protoka vazduha od 1 m/s i temperaturi od 30 °C–50 °C. Statistička analiza je pokazala da je Verma jednačina najbolje prilagođen model sa najnižim hi-kvadrat i AIC vrednostima na svim temperaturama. Iz statističkih analiza korišćenjem razvijenih modela sušenja, otkriveno je da je D9 jednačina koja ima vrednost hi-kvadrat od 0,0146 i AIC vrednost od -528,0, najbolje slaganje modela sa eksperimentalnim podacima. Ukupan sadržaj fenola, flavonoida i antioksidativni kapacitet uzoraka osušenog bosiljka izmeren je kao (2,538 ± 0,029) mg GAE/g, (2,017 ± 0,088) mg kvercetina/g i (2,263 ± 0,001) mmol TEAC/100 g, redom. FTIR spektri pokazuju da su uzorci osušenog bosiljka imali tipične funkcionalne grupe. SEM slike su pokazale da je došlo do kolapsa na površini listova. Ali, ovaj kolaps ne utiče na funkcionalne grupe na površini listova. Iz analize potrošnje energije, utvrđeno je da je optimalna temperatura sušenja 40 °C. Vrednosti SMER, MER i SEC izračunate iz analize potrošnje energije na 40 °C bile su 0,0043 kg/kVh, 0,0007 kg/h i 234,81 kVh/kg, redom.*

*Ključne reči: mikropropagacija, *O. basilicum* L., sušenje u tankom sloju, modelovanje, karakteristika, potrošnja energije.*